Synthesis of atom-specific nucleobase and ribose labeled uridine phosphoramidite for NMR analysis of large RNAs

Lukasz Olenginski[1] ● Owen Becette[2] ● Serge L. Beaucage[3] ● Theodore K. Dayie[1]

Received: ……/Accepted …

Abstract We describe the hybrid enzymatic and chemical synthesis of a 2′-O-cyanoethoxymethyl (CEM) [1′,6-$^{13}C_2$, 5-^{2}H]-uridine phosphoramidite (amidite). This is the first report of an atom-specific nucleobase and ribose labeled CEM amidite. Importantly, the CEM 2′-OH protecting group permits the efficient solid-phase synthesis of large (>60 nucleotides) RNAs with good yield and purity. Therefore, our isotope-labeled amidite can be used to make large, position-specifically labeled RNAs for NMR analysis without complications from resonance overlap and scalar and dipolar couplings.

Keywords Isotopic labeling ● Nucleic acids ● RNA ● Synthesis

✉ Theodore K. Dayie
dayie@umd.edu

[1] Center for Biomolecular Structure and Organization, Department of Chemistry and Biochemistry, University of Maryland, College Park, MD 20742, United States.

[2] Institute for Bioscience and Biotechnology Research, National Institute of Standards and Technology and the University of Maryland, Rockville, Maryland 20850, United States.

[3] Laboratory of Biological Chemistry, Division of Biotechnology Review and Research IV, Center for Drug Evaluation and Research, Food and Drug Administration, 10903 New Hampshire Avenue, Silver Spring, Maryland 20933, United States.

Introduction

Nuclear magnetic resonance (NMR) spectroscopy is a biophysical method well suited to study RNA structure, dynamics, and interactions at high-resolution [1–3]. Many contemporary NMR experiments require the introduction of stable isotope (e.g., ^{13}C, ^{19}F, ^{2}H, and ^{15}N) labels into RNA [4–6]. This is routinely accomplished with T7 RNA polymerase-based *in vitro* transcription [7]. By mixing labeled and unlabeled ribonucleoside 5′-triphosphates (rNTPs), this technique permits uniform, nucleotide-, and/or atom-specific labeling (Fig. 1a-c). Some of these labeled rNTP precursors are commercially available, and the synthetic routes to many more exist in the literature [8–20]. Although this method produces RNA in yields amenable to NMR analysis, resonance overlap presents a significant problem for large RNAs (>60 nucleotides, nts). To overcome this limitation, alternative RNA labeling methods must be used.

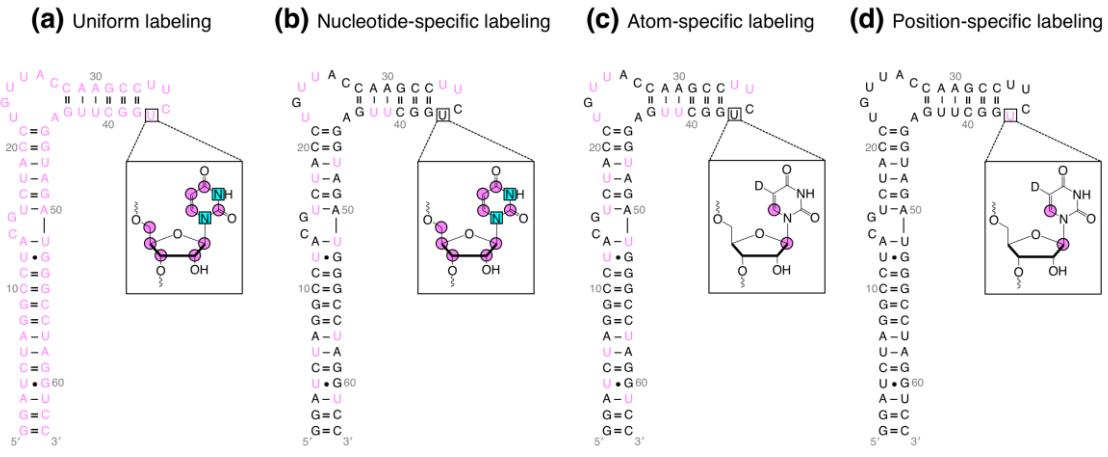

Fig. 1 Schematic of a 63 nt RNA that is either **a** uniformly, **b** nucleotide-specifically, **c** atom-specifically, or **d** position-specifically labeled. The RNAs in **a-c** can be prepared by *in vitro* transcription using either uniformly ^{13}C- and ^{15}N-labeled rNTPs, uniformly ^{13}C- and ^{15}N-labeled UTP, or [1′,6-$^{13}C_2$, 5-^{2}H]-UTP, respectively. The RNA in **d** can be prepared by solid-phase synthesis with a [1′,6-$^{13}C_2$, 5-^{2}H]-uridine amidite. Pink residues are isotope-labeled. Pink circles, cyan squares, and D represent ^{13}C, ^{15}N, and ^{2}H atoms, respectively.

One such technique employs isotope-labeled 2′-O-triisopropylsilyloxymethyl (TOM)- or 2′-O-*tert*-butyldimethylsilyl (TBDMS) ribonucleoside phosphoramidites (amidites) and solid-phase synthesis [21–25]. This method allows users to choose the site(s) of modification and therefore enables position-specific labeling (Fig. 1d). As with rNTPs, some labeled amidite precursors are available from commercial

sources, and synthetic access to many others is well documented [21–25]. Solid-phase synthesis works well for medium sized RNAs (20-50 nt), but standard methodologies are not apt to produce RNAs >60 nt with the yield and purity required for NMR analysis [26–30]. To overcome this limitation, Kreutz and co-workers established an improved synthetic procedure [31] to make labeled 2′-O-cyanoethoxymethyl (CEM) amidites [32–34]. While these precursors (labeled or unlabeled) are commercially unavailable, they offer improved coupling efficiency [32–34] and are therefore the only amidites capable of synthesizing large RNAs for NMR applications.

Although the synthesis of [8-^{13}C]-adenosine and -guanosine and [6-^{13}C, 5-^{2}H]-cytidine and -uridine CEM amidites are known (Fig. 2) [31], the labeling of both nucleobase and ribose moieties has yet to be implemented into such precursors. Our recent work in collaboration with Kreutz and co-workers [21] demonstrated initial success in this direction. Here, we combined chemo-enzymatic nucleobase and ribose coupling [19] with chemical synthesis to produce an [1′,8-$^{13}C_2$]-adenosine TBDMS amidite (Fig. 2) [21]. This hybrid approach is beneficial because it permits the incorporation of isolated ^{1}H-^{13}C spin pairs into the nucleobase and ribose to facilitate unambiguous resonance assignment. In addition, the removal of ^{13}C-^{13}C scalar and dipolar coupling benefit NMR dynamics experiments [35–37]. Here, we detail a combined enzymatic and chemical method to

synthesize [1′,6-$^{13}C_2$, 5-^{2}H]-uridine CEM amidite (Fig. 2). Importantly, this precursor can be used in solid-phase synthesis to produce large, position-specifically labeled RNAs amenable for NMR analysis.

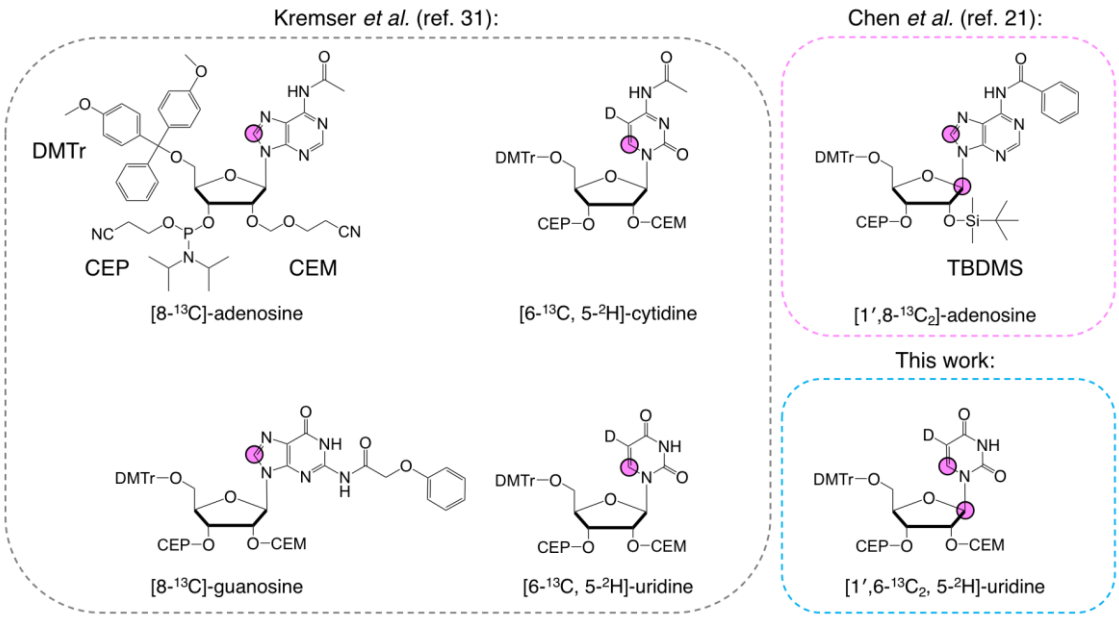

Fig. 2 Examples of previously prepared isotope-labeled CEM [31] and TBDMS amidites [21], as well as the featured nucleobase and ribose labeled CEM amidite of the present study. Pink circles and D represent ^{13}C and ^{2}H atoms, respectively.

Results and discussion

Synthesis

The atom-specific nucleobase and ribose labeled [1′,6-$^{13}C_2$, 5-^{2}H]-uridine CEM amidite **6** was assembled with a hybrid enzymatic (Scheme 1) and chemical (Scheme 2) approach. First, we used enzymes from the nucleotide salvage biosynthetic pathways [38] to couple [6-^{13}C, 5-^{2}H]-uracil (prepared as previously described [39]) with commercially available [1-^{13}C]-D-ribose. This one-pot reaction was used modifying our previously published procedure [20, 21]. In brief, ribokinase (RK, E.C. 2.7.1.15) phosphorylates the O5 position of [1-^{13}C]-D-ribose and then phosphoribosyl pyrophosphate synthetase (PRPPS, E.C. 2.7.6.1) pyrophosphorylates the $^{13}C1$ site. Uracil phosphoribosyl transferase (UPRT, E.C. 2.4.2.9) then couples [6-^{13}C, 5-^{2}H]-uracil to the 5-phospho-D-ribosyl-α-1-pyrophosphate intermediate via nucleophilic attack of uracil N1. In the final enzymatic step, the uridine 5′-monophosphate (UMP) intermediate was dephosphorylated with recombinant shrimp alkaline phosphatase (rSAP, E.C.3.1.3.1) to yield [1′,6-$^{13}C_2$, 5-^{2}H]-uridine **1** (Scheme 1).

Scheme 1

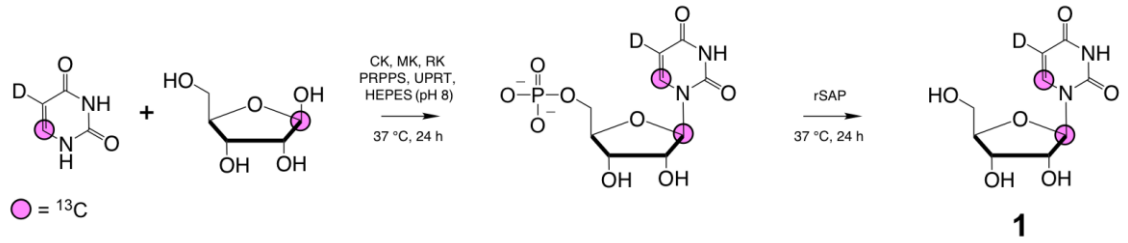

Our atom-specific labeled uridine **1** was then used as the starting point to chemically synthesize the desired CEM amidite following established protocols [31–34]. To ensure selective 2′-O-alkylation, we first protected the 3′- and 5′-OH groups of **1** with 1,3-dichloro-1,1,3,3-tetraisopropyldisiloxane (TIPS-Cl_2) to yield 3′,5′-*di*-O-protected uridine **2**. Subsequent reaction of **2** with 2-cyanoethyl methylthiomethylether (C_5H_9NOS, prepared as previously described [32]) as the alkylating agent and N-iodosuccinimide (NIS) as the activator led to efficient production of 2′-O-CEM uridine **3** at low temperature (-45 °C). Treatment of **3** with ammonium fluoride led to removal of the 3′,5′-di-O-TIPS group to yield **4**. In the second to last step, the 5′-OH group of **4** was tritylated with 4,4′-dimethoxytrityl chloride (DMTr) to form **5**. Lastly, phosphitylation of **5** yielded the desired [1′,6-$^{13}C_2$, 5-^{2}H]-5′-O-DMTr-2′-O-CEM amidite **6** (Scheme 2). Pure intermediate compounds **2** and **5** as well as the desired compound **6** displayed the expected ^{1}H and ^{13}C NMR spectra reported in the literature [31–34]. ^{31}P NMR also confirmed our amidite **6**, albeit with some phosphonate impurity.

In summary, our synthetic route provides **6** with an overall yield of 8.4% with two enzymatic steps (Scheme 1), five chemical steps (Scheme 2), and four chromatographic purifications. This is the first report of an atom-specific nucleobase and ribose labeled CEM amidite. Moreover, our

approach permits the production of additional atom-specific labeling patterns by coupling different commercially available or in-house synthesized ^{2}H-, ^{13}C-, and/or ^{15}N-labeled nucleobases to commercial sources of ^{2}H and/or ^{13}C-labeled D-ribose.

Scheme 2

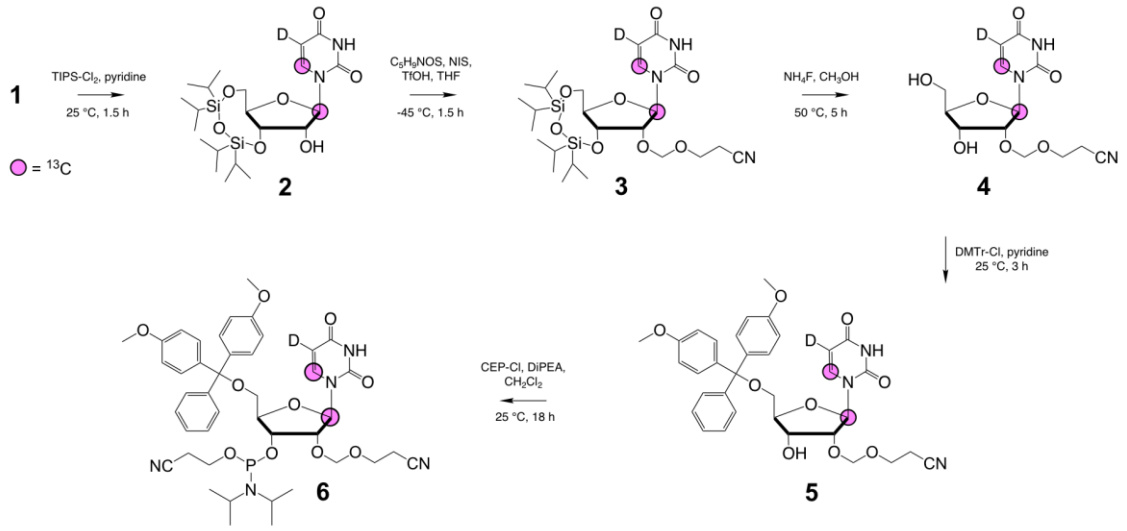

Future application

Our motivation to synthesize CEM amidite **6** was for NMR analysis of large RNAs. The CEM 2′-OH protecting group has minimal steric demands and a clean deprotection procedure [32–34]. Taken together, CEM amidites have increased coupling efficiency that enables the synthesis of large RNAs [32–34]. Therefore, mixing unlabeled CEM amidites with our newly synthesized

6 can permit the rapid construction of strategically labeled RNAs. These samples can then be used for unambiguous nucleobase H6-C6 and ribose H1′-C1′ resonance assignments and ^{13}C NMR relaxation and/or relaxation dispersion probing of nucleobase C6 and ribose C1′ nuclei.

Conclusion

We report the enzymatic and chemical synthesis of the first atom-specific nucleobase and ribose labeled [1′,6-$^{13}C_2$, 5-^{2}H]-uridine CEM amidite. The isotope-labeled uridine was synthesized in a one-pot, two-step enzymatic reaction from [6-^{13}C, 5-^{2}H]-uracil and commercially available [1-^{13}C]-D-ribose. The nucleoside intermediate was then chemically built into the desired CEM amidite. Future applications include the position-specific incorporation of our amidite into large RNAs via solid-phase synthesis and subsequent NMR analysis.

Experimental

Commercially available reagents were used throughout without further purification. All non-commercial enzymes used were expressed and purified in-house [38]. [6-^{13}C, 5-^{2}H]-uracil [39] and alkylating agent 2-cyanoethyl methylthiomethylether [32] were both prepared following previously

established protocols. [1-^{13}C]-D-ribose was purchased from Omicron Scientific. All solvents were obtained as spectroscopic grade and used as received. All reactions sensitive to air and/or moisture were carried out under an atmosphere of argon in anhydrous solvents using oven-dried glassware. Thin-layer chromatography (TLC) was performed using aluminum plates coated with silica gel 60 F-254. Chromatographic purifications were carried out using a boronate affinity resin or silica gel with eluent specified. Mass spectrometric data were collected on a PerkinElmer AXION 2 TOF mass spectrometer with APCI source using ESI negative mode. ^{1}H and ^{13}C NMR spectra were recorded on a Bruker DRX 300 MHz spectrometer. Samples were maintained at a temperature of 25 °C. All spectra were recorded in deuterated solvents and chemical shifts δ are reported in parts per million (ppm) relative to appropriate internal references. The following abbreviations were used to denote multiplicities: s singlet, d doublet, t triplet, m multiplet, b broad.

Synthesis

^{1}H and ^{13}C NMR spectra of compounds **2**, **5**, and **6** and ^{31}P NMR spectra and high-resolution mass spectrometry (HRMS) data for **6** can be found in the Supplemental Material.

[1′,6-$^{13}C_2$, 5-^{2}H]-1-((2*R*,3*R*,4*S*,5*R*)-3,4-dihydroxy-5-(hydroxymethyl)tetrahydrofuran-2-yl)pyrimidine-2,4(1*H*,3*H*)-dione (1, $C_7{}^{13}C_2H_{11}{}^{2}HN_2O_6$)

Compound **1** was enzymatically synthesized *in vitro*. The 200 cm^3 reaction was carried out in 50 mM HEPES pH 8, 0.2% NaN_3, 10 mM $MgCl_2$, 10 mM DTT, 0.5 mM dATP, 0.1% BSA, 100 mM creatine phosphate, 10 mM [6-^{13}C, 5-^{2}H]-uracil, 8 mM [1-^{13}C]-D-ribose, 0.005 mg/cm^3 CK (E.C. 2.7.3.2), 0.01 U/cm^3 myokinase (MK, E.C. 2.7.4.3), 0.1 mg/cm^3 thermostable inorganic pyrophosphatase (TIPP, E.C. 3.6.1.1), 1x10^{-5} U/mm^3 RK (E.C. 2.7.1.15), 1x10^{-5} U/mm^3 PRPPS (E.C. 2.7.6.1), and 0.1 mg/cm^3 UPRT (E.C. 2.4.2.9). The reaction was split into five 40 cm^3 aliquots and incubated at 37 °C for 24 h. The monophosphate product was converted into crude compound **1** by adding rSAP (E.C.3.1.3.1) (1.81 mm^3/per reaction cm^3) and incubating at 37 °C for an additional 24 h. Crude compound **1** was purified by boronate affinity chromatography (Eluent A: 1 M TEABC pH 9; Eluent B: acidified water pH 4) and lyophilized to an off-white oil. Finally, the oil was dissolved ($CHCl_3$/CH_3OH = 1/1 (v/v)) and purified via column chromatography (7.5 g SiO_2, ($CHCl_3$/CH_3OH = 9/1 (v/v))) to yield pure compound **1** as a white foam after drying under high vacuum. Yield: 351 mg

(~80% to input uracil for each 40 cm^3 aliquot); R_f: 0.75 ($CHCl_3/CH_3OH$ = 3/2 (v/v)). ^1H NMR: not determined; ^{13}C NMR: not determined.

[1′,6-$^{13}C_2$, 5-^2H]-1-((6a*R*,8*R*,9*R*,9a*S*)-9-hydroxy-2,2,4,4-tetraisopropyltetrahydro-6*H*-furo[3,2 *f*][1,3,5,2,4]trioxadisilocin-8-yl)pyrimidine-2,4(1*H*,3*H*)-dione (2, $C_{19}{}^{13}C_2H_{37}{}^2H\ N_2O_7Si_2$)

Compound **1** (351 mg, 1.42 mmol, 1.00 eq.) was co-evaporated with anhydrous pyridine and then dissolved in fresh anhydrous pyridine (1.81 cm^3). Then, 1,3-dichloro-1,1,3,3-tetraisopropyldisiloxane (TIPS-Cl_2, 500 mg, 1.59 mmol, 1.10 eq.) was added dropwise over 60 min and the reaction mixture was stirred under argon atmosphere at room temperature for an additional 30 min. After TLC ($CHCl_3$/MeOH = 9/1 (v/v)) showed a complete conversion, the solution was diluted with saturated sodium bicarbonate (20 cm^3) and the solution was extracted with dichloromethane (20 cm^3). The organic phase was dried over anhydrous sodium sulfate and the solution was evaporated to dryness. The residual oil was co-evaporated with anhydrous toluene twice and dried under high vacuum. Crude product **2** was purified via column chromatography (6.5 g, SiO_2, ($CHCl_3/CH_3CN$ = 100/0 – 80/20 (v/v))) to obtain pure compound **2** as a white foam after drying under high vacuum. Yield: 271 mg (39%); R_f: 0.46; ^1H NMR (300 MHz, DMSO-d_6): δ = 11.35 (s, 1H, N(3)H); 7.98 (d, $^1J_{H6C6}$ = 181.43 Hz, 1H, $^{13}C(6)H$); 5.82 (d,

$^{1}J_{H1'C1'}$ = 173.11 Hz, 1H, ^{13}C(1′)H); 5.58 (d, $^{3}J_{HH}$ = 9.17 Hz, 1H, C(2′)OH); 4.28 – 4.11 (m, 3H, C(2′)H; C(3′)H; C(4′)H); 3.98 – 3.89 (m, 2H, C(5′)H; C(5″)H); 1.05 – 0.97 (m, 28H, 4xSi-CH-$(CH_3)_2$; 4xSi-CH-$(CH_3)_2$); ^{13}C NMR (75 MHz, DMSO-d_6): δ = 140.21(^{13}C(6)); 90.99 (^{13}C(1′)).

[1′,6-$^{13}C_2$, 5-^{2}H]-3-((((6a*R*,8*R*,9*R*,9a*R*)-8-(2,4-dioxo-3,4-dihydropyrimidin-1(2*H*)-yl)-2,2,4,4-tetraisopropyltetrahydro-6*H*-furo[3,2-*f*][1,3,5,2,4]trioxadisilocin-9-yl)oxy)methoxy)propanenitrile (3, $C_{23}{}^{13}C_2H_{42}{}^{2}HN_3O_8Si_2$)

Compound **2** (260 mg, 0.53 mmol, 1.00 eq.) was dissolved in anhydrous tetrahydrofuran (THF, 4 cm^3) and 2-cyanoethyl methylthiomethylether (C_5H_9NOS, 146 mg, 1.12 mmol, 2.10 eq.) was added. The solution was cooled to -45 °C with a dry ice/acetonitrile bath and stirred under argon atmosphere for 30 min. Trifluoromethanesulfonic acid (TfOH, 167 mg, 1.12 mmol, 2.10 eq.) was carefully dropped into the mixture over a period of 10 min and then N-iodosuccinimide (NIS, 113 mg, 1.12 mmol, 2.10 eq.) was added in one portion. The reaction mixture was stirred for 15 min at -45 °C and then triethylamine (113 mg, 1.12 mmol, 2.10 eq.) was slowly added over a period of 20 min to quench the reaction. The mixture was diluted with ethyl acetate (10 cm^3) and washed with saturated sodium thiosulfate (10 cm^3) and saturated sodium bicarbonate solution (10 cm^3). The organic layers were

evaporated to dryness and the residual oil was dissolved in ethyl acetate (10 cm^3). The mixture was successively washed with water (10 cm^3), saturated sodium thiosulfate (10 cm^3), and saturated sodium chloride (10 cm^3). The organic layer was dried over anhydrous sodium sulfate and the solution was evaporated to dryness. The residual light brown oil was isolated as crude compound **3** and dried under high vacuum. No further purification steps were used and the crude product **3** was used in the next synthetic step. Yield: assumed to be 304 mg (100%); R_f: 0.52 ($CHCl_3/CH_3OH$ = 9/1 (v/v)); ^{1}H-NMR: not determined; ^{13}C NMR: not determined.

[1′,6-$^{13}C_2$, 5-^{2}H]-3-((((2*R*,3*R*,4*R*,5*R*)-2-(2,4-dioxo-3,4-dihydropyrimidin-1(2*H*)-yl)-4-hydroxy-5-(hydroxymethyl)tetrahydrofuran-3-yl)oxy)methoxy)propanenitrile (4, $C_{11}{}^{13}C_2H_{16}{}^2HN_3O_7$)

Crude compound **3** (304 mg, 0.53 mmol, 1.00 eq.) was dissolved in anhydrous methanol (CH_3OH, 7.5 cm^3) and ammonium fluoride (NH_4F, 72.2 mg, 1.95 mmol, 3.67 eq.) was added. The reaction mixture was heated to 50 °C and stirred for 5 h under argon atmosphere. After TLC (CH_3Cl/CH_3OH = 9/1 (v/v)) showed complete conversion, methanol was removed under reduced pressure. The residue was dissolved in acetonitrile (10 cm^3) and the white precipitate that formed was removed by vacuum filtration and washed with acetonitrile. The solution was extracted with n-hexane twice, the hexane

layers were discarded, the acetonitrile layer was dried over anhydrous sodium sulfate, and the solution was evaporated to dryness. The residual oil was isolated as crude compound **4** and dried under high vacuum. No further purification steps were used and the crude product **4** was used in the next synthetic step. Yield: assumed to be 175 mg (100%); R_f = 0.18 ($CHCl_3$/CH_3OH = 9/1 (v/v)); ^{1}H-NMR: not determined; ^{13}C NMR: not determined.

[1′,6-$^{13}C_2$, 5-^{2}H]-3-((((2*R*,3*R*,4*R*,5*R*)-5-((bis(4-methoxyphenyl)(phenyl)methoxy)methyl)-2-(2,4-dioxo-3,4-dihydropyrimidin-1(2*H*)-yl)-4-hydroxytetrahydrofuran-3-yl)oxy)methoxy)propanenitrile (5, $C_{32}{}^{13}C_2H_{34}{}^2HN_3O_9$)

Crude compound **4** (175 mg, 0.53 mmol, 1.00 eq.) was co-evaporated with anhydrous pyridine and then dissolved in fresh anhydrous pyridine (3.5 cm^3). Then, 4,4'-dimethoxytrityl chloride (DMTr, 215 mg, 0.64 mmol, 1.20 eq.) was added with stirring at room temperature under argon atmosphere (3 h). After TLC (CH_3Cl/CH_3OH = 9/1 (v/v)) showed complete conversion, the reaction was quenched with cold water (10 cm^3) and extracted with chloroform (10 cm^3) twice. The organic phase was dried over anhydrous sodium sulfate and the solution was evaporated to dryness and dried under high vacuum. The crude product **5** was purified via column chromatography

(6.0 g, SiO_2, ((CH_3Cl/CH_3OH = 100/0 – 98/2 (v/v)) + 0.5% pyridine) to obtain pure compound **5** as an off-white solid. Yield: 200 mg (60%); R_f = 0.33 ($CHCl_3/CH_3OH$ = 9/1 (v/v)); ^{1}H NMR (300 MHz, DMSO-d_6): δ = 11.39 (s, 1H, N(3)H); 8.04 (d, $^1J_{H6C6}$ = 181.75 Hz, 1H, ^{13}C(6)H); 7.40 – 7.14 (m, 9H, arom. CH); 6.92 – 6.89 (d, $^3J_{HH}$ = 8.98 Hz, 4H, arom. CH-C-OCH_3); 5.50 (d, $^1J_{H1'C1'}$ = 170.37 Hz, 1H, ^{13}C(1′)H); 5.37 (d, $^3J_{HH}$ = 6.22 Hz, 1H, C(3′)OH); 4.83 (s, 2H, -O-CH_2-O-); 4.26 – 4.24 (m, 2H, C(2′)H; C(3′)H); 3.98 (singlettoid, 1H, C(4′)H); 3.744 (s, 6H, 2x -OCH_3); 3.70 – 3.64 (m, 2H, -O-CH_2-CH_2-); 3.33 – 3.21 (m, 2H, C(5′)H; C(5″)H); 2.79 (dd, $^2J_{HH}$ = 15.86, $^3J_{HH}$ = 3.92, 2H, -O-CH_2-CH_2); ^{13}C NMR (75 MHz, DMSO-d_6): δ = 140.55 (^{13}C(6)); 87.98 (^{13}C(1′)).

[1′,6-$^{13}C_2$, 5-^{2}H]-(2*R*,3*R*,4*R*,5*R*)-2-((bis(4-methoxyphenyl)(phenyl)methoxy)methyl)-4-((2-cyanoethoxy)methoxy)-5-(2,4-dioxo-3,4-dihydropyrimidin-1(2*H*)-yl)tetrahydrofuran-3-yl (2-cyanoethyl) diisopropylphosphoramidite (6, $C_{41}{}^{13}C_2H_{51}{}^2HN_5O_{10}P$)

Compound **5** (195 mg, 0.31 mmol, 1.00 eq.) was dissolved in anhydrous dichloromethane (3 cm^3). Then, both N,N-Diisopropylethylamine (DiPEA, 119 mg, 0.92 mmol, 3.00 eq.) and 2′-cyanoethyl-N,N-diisopropylchlorophosphoramidite (CEP-Cl, 109 mg, 0.46 mmol, 1.5 eq.)

were added and the solution was stirred overnight (~16-18 h). Monitoring with TLC (CH_3Cl/CH_3OH = 9/1 (v/v)) showed some unreacted starting material, so 0.5 additional eq. of CEP-Cl were added, and the solution was stirred until TLC (CH_3Cl/CH_3OH = 9/1 (v/v)) showed complete conversion (~1 h). The reaction was quenched with water (10 cm^3) and the solution was extracted with dichloromethane (10 cm^3) twice. The organic phase was dried over anhydrous sodium sulfate and the solution was evaporated to dryness and dried under high vacuum. The crude product **6** was purified via column chromatography (7.5 g, SiO_2, (benzene/TEA = 9/1 (v/v)) to obtain pure compound **6** as a white foam consisting of a mixture of two diastereomers after drying under high vacuum. Yield: 120 mg (45%); R_f = 0.54 + 0.58 ($CHCl_3/CH_3OH$ = 9/1 (v/v)); ^{1}H NMR (300 MHz, DMSO-d_6): δ = 11.38 (s, 1H, N(3)H); 8.06 (d, $^1J_{H6C6}$ = 181.75 Hz, 1H, ^{13}C(6)H); 7.38 – 7.23 (m, 9H, arom. CH); 6.92 – 6.88 (d, $^3J_{HH}$ = 11.51 Hz, 4H, arom. CH-C-OCH_3); 6.14 (d, $^1J_{H1'C1'}$ = 169.46 Hz, 1H, ^{13}C(1′)H); 4.85 – 4.79 (m, 2H, -O-CH_2-O-); 4.43 – 4.40 (m, 2H, C(3′)H), C(2′)H); 4.13 – 3.99 (m, 2H, C(4′)H), -P-O-CH'_2-CH_2-); 3.74 (s, 6H, 2x -OCH_3); 3.73 – 3.69 (m, 2H, -P-O-CH''_2-CH_2-; -CH_2-O-CH'_2-CH_2-); 3.55 – 3.41 (m, 3H, C(5′)H; C(5″)H; -CH_2-O-CH''_2-CH_2-); 2.80 – 2.73 (m, 2H, -P-O-CH_2-CH_2-; -CH_2-O-CH_2-CH'_2-); 2.64 – 2.60 (m, 1H, -CH_2-O-CH_2-CH''_2-); 1.24 – 1.08 (m, 14H 2x -N-CH-$(CH_3)_2$; 2x -N-CH-$(CH_3)_2$); ^{13}C NMR (75 MHz, DMSO-d_6): δ = 140.71 (^{13}C(6)); 88.49 (^{13}C(1′));

^{31}P NMR: (122 MHz, C_6D_6): δ = 151.33 (s); 149.62 (s); HRMS (ESI): *m/z* calculated for $C_{41}{}^{13}C_2H_{51}{}^{2}HN_5O_{10}P$ $[M^-H]^-$ 831.3498 Da, found 831.3481 Da.

Acknowledgements This research was financially supported by NSF for labeling work (1808705 to T.K.D.). We acknowledge Drs. Harsh V. Jain and Andrzej Grajkowski (FDA) for helpful supervision of the synthetic work and Joshua Wilhide (UMBC) for mass spectrometric analysis.

References

1. Thompson RD, Baisden JT, Zhang Q (2019) NMR characterization of RNA small molecule interactions. Methods 167:66–77. https://doi.org/10.1016/j.ymeth.2019.05.015
2. Marušič M, Schlagnitweit J, Petzold K (2019) RNA Dynamics by NMR Spectroscopy. ChemBioChem 20:2685–2710. https://doi.org/10.1002/cbic.201900072
3. Barnwal RP, Yang F, Varani G (2017) Applications of NMR to structure determination of RNAs large and small. Arch Biochem Biophys 628:42–56. https://doi.org/10.1016/j.abb.2017.06.003
4. Marchanka A, Kreutz C, Carlomagno T (2018) Isotope labeling for

studying RNA by solid-state NMR spectroscopy. J Biomol NMR 71:151–164. https://doi.org/10.1007/s10858-018-0180-7

5. Asadi-Atoi P, Barraud P, Tisne C, Kellner S (2019) Benefits of stable isotope labeling in RNA analysis. Biol Chem 400:847–865. https://doi.org/10.1515/hsz-2018-0447

6. Becette O, Olenginski LT, Dayie TK (2019) Solid-phase chemical synthesis of stable isotope-labeled RNA to aiD structure and dynamics studies by NMR spectroscopy. Molecules 24:3476. https://doi.org/10.3390/molecules24193476

7. Milligan JF, Uhlenbeck OC (1989) Synthesis of small RNAs using T7 RNA polymerase. Methods Enzymol 180:51–62. https://doi.org/10.1016/0076-6879(89)80091-6

8. Schultheisz HL, Szymczyna BR, Scott LG, Williamson JR (2011) Enzymatic de novo pyrimidine nucleotide synthesis. J Am Chem Soc 133:297–304. https://doi.org/10.1021/ja1059685

9. Schultheisz HL, Szymczyna BR, Scott LG, Williamson JR (2008) Pathway engineered enzymatic de novo purine nucleotide synthesis. ACS Chem Biol 3:499–511. https://doi.org/10.1021/cb800066p

10. Tolbert TJ, Williamson JR (1996) Preparation of specifically deuterated RNA for NMR studies using a combination of chemical and enzymatic synthesis. J Am Chem Soc 118:7929–7940.

https://doi.org/10.1021/ja961274i

11. Johnson JE, Julien KR, Hoogstraten CG (2006) Alternate-site isotopic labeling of ribonucleotides for NMR studies of ribose conformational dynamics in RNA. J Biomol NMR 35:261–274. https://doi.org/10.1007/s10858-006-9041-x

12. Hoffman DW, Holland JA (1995) Preparation of carbon-13 labeled ribonucleotides using acetate as an isotope source. Nucleic Acids Res 23:3361–3362. https://doi.org/10.1093/nar/23.16.3361-b

13. Thakur CS, Dayie TK (2012) Asymmetry of ^{13}C labeled 3-pyruvate affords improved site specific labeling of RNA for NMR spectroscopy. J Biomol NMR 52:65–77. https://doi.org/10.1007/s10858-011-9582-5

14. Thakur CS, Sama JN, Jackson ME, et al (2010) Selective ^{13}C labeling of nucleotides for large RNA NMR spectroscopy using an E. coli strain disabled in the TCA cycle. J Biomol NMR 48:179–192. https://doi.org/10.1007/s10858-010-9454-4

15. Scott LG, Geierstanger BH, Williamson JR, Hennig M (2004) Enzymatic synthesis and 19F NMR studies of 2-fluoroadenine-substituted RNA. J Am Chem Soc 126:11776–11777. https://doi.org/10.1021/ja047556x

16. Hennig M, Scott LG, Sperling E, et al (2007) Synthesis of 5-fluoropyrimidine nucleotides as sensitive NMR probes of RNA

structure. J Am Chem Soc 129:14911–14921. https://doi.org/10.1021/ja073825i

17. Olenginski LT, Dayie TK (2020) Chemo-enzymatic synthesis of [2-^{13}C, 7-^{15}N]-ATP for facile NMR analysis of RNA. Monatshefte fur Chemie 151:1467–1473. https://doi.org/10.1007/s00706-020-02667-6

18. Taiwo KM, Becette OB, Zong G, et al (2021) Chemo-enzymatic synthesis of ^{13}C- and ^{19}F-labeled uridine-5′-triphosphate for RNA NMR probing. Monatshefte für Chemie - Chem Mon 152:441–447. https://doi.org/10.1007/s00706-021-02757-z

19. Longhini AP, Leblanc RM, Becette O, et al (2015) Chemo-enzymatic synthesis of site-specific isotopically labeled nucleotides for use in NMR resonance assignment, dynamics and structural characterizations. Nucleic Acids Res 44:. https://doi.org/10.1093/nar/gkv1333

20. Alvarado LJ, Leblanc RM, Longhini AP, et al (2014) Regio-selective chemical-enzymatic synthesis of pyrimidine nucleotides facilitates RNA structure and dynamics studies. ChemBioChem 15:1573–1577. https://doi.org/10.1002/cbic.201402130

21. Chen B, Longhini AP, Nußbaumer F, et al (2018) CCR5 RNA Pseudoknots: Residue and Site-Specific Labeling correlate Internal Motions with microRNA Binding. Chem - A Eur J 24:5462–5468.

https://doi.org/10.1002/chem.201705948

22. Neuner S, Santner T, Kreutz C, Micura R (2015) The “speedy” Synthesis of Atom-Specific ^{15}N Imino/Amido-Labeled RNA. Chem - A Eur J 21:11634–11643. https://doi.org/10.1002/chem.201501275

23. Wunderlich CH, Spitzer R, Santner T, et al (2012) Synthesis of (6-^{13}C)pyrimidine nucleotides as spin-labels for RNA dynamics. J Am Chem Soc 134:7558–7569. https://doi.org/10.1021/ja302148g

24. Neuner S, Kreutz C, Micura R (2017) The synthesis of ^{15}N(7)-Hoogsteen face-labeled adenosine phosphoramidite for solid-phase RNA synthesis. Monatshefte fur Chemie 148:149–155. https://doi.org/10.1007/s00706-016-1882-8

25. Juen MA, Wunderlich CH, Nußbaumer F, et al (2016) Excited States of Nucleic Acids Probed by Proton Relaxation Dispersion NMR Spectroscopy. Angew Chemie - Int Ed 55:12008–12012. https://doi.org/10.1002/anie.201605870

26. Muller S, Wolf J, Ivanov S (2005) Current Strategies for the Synthesis of RNA. Curr Org Synth 1:293–307. https://doi.org/10.2174/1570179043366675

27. Somoza, Àlvaro S (2008) Protecting groups for RNA synthesis: An increasing need for selective preparative methods. Chem Soc Rev 37:2668–2675. https://doi.org/10.1039/b809851d

28. Reese CB (2002) The chemical synthesis of oligo- and poly-nucleotides: A personal commentary. Tetrahedron 58:8893–8920. https://doi.org/10.1016/S0040-4020(02)01084-0

29. Scaringe SA, Wincott FE, Caruthers MH (1998) Novel RNA synthesis method using S'-O-silyl-2'-O-orthoester protecting groups [13]. J Am Chem Soc 120:11820–11821. https://doi.org/10.1021/ja980730v

30. Beaucage SL, Caruthers MH (1981) Deoxynucleoside phosphoramidites-A new class of key intermediates for deoxypolynucleotide synthesis. Tetrahedron Lett 22:1859–1862. https://doi.org/10.1016/S0040-4039(01)90461-7

31. Kremser J, Strebitzer E, Plangger R, et al (2017) Chemical synthesis and NMR spectroscopy of long stable isotope labelled RNA. Chem Commun 53:12938–12941. https://doi.org/10.1039/c7cc06747j

32. Ohgi T, Masutomi Y, Ishiyama K, et al (2005) A new RNA synthetic method with a 2′-O-(2-cyanoethoxymethyl) protecting group. Org Lett 7:3477–3480. https://doi.org/10.1021/ol051151f

33. Masuda H, Shiba Y, Watanabe N, et al (2007) Chemical synthesis of a very long RNA oligomer, a 110mer precursor-miRNA candidate, with 2-cyanoethoxymethyl (CEM) as the 2'-O-protecting group. Nucleic Acids Symp Ser (Oxf) 3–4. https://doi.org/10.1093/nass/nrm002

34. Ohgi T, Kitagawa H, Yano J (2008) Chemical synthesis of

oligoribonucleotides with 2′-O-(2-cyanoethoxymethyl)-protected phosphoramidites. Curr. Protoc. Nucleic Acid Chem. 34:2.15.1-2.15.19

35. Olenginski LT, Dayie TK (2021) Quantifying the effects of long-range ^{13}C-^{13}C dipolar coupling on measured relaxation rates in RNA. J Biomol NMR 75:203–211. https://doi.org/10.1007/s10858-021-00368-8

36. Nam H, Becette O, LeBlanc RM, et al (2020) Deleterious effects of carbon–carbon dipolar coupling on RNA NMR dynamics. J Biomol NMR 74:321–331. https://doi.org/10.1007/s10858-020-00315-z

37. Yamazaki T, Muhandiram R, Kay LE (1994) NMR Experiments for the Measurement of Carbon Relaxation Properties in Highly Enriched, Uniformly ^{13}C,^{15}N-Labeled Proteins: Application to $^{13}C^{\alpha}$Carbons. J Am Chem Soc 116:8266–8278. https://doi.org/10.1021/ja00097a037

38. Arthur PK, Alvarado LJ, Dayie TK (2011) Expression, purification and analysis of the activity of enzymes from the pentose phosphate pathway. Protein Expr Purif 76:229–237. https://doi.org/10.1016/j.pep.2010.11.008

39. Juen MA, Wunderlich CH, Nußbaumer F, et al (2016) Excited States of Nucleic Acids Probed by Proton Relaxation Dispersion NMR Spectroscopy. Angew Chemie - Int Ed 55:12008–12012.

https://doi.org/10.1002/anie.201605870

Figure Captions

Fig. 1 Schematic of a 63 nt RNA that is either **a** uniformly, **b** nucleotide-specifically, **c** atom-specifically, or **d** position-specifically labeled. The RNAs in **a-c** can be prepared by *in vitro* transcription using either uniformly ^{13}C- and ^{15}N-labeled rNTPs, uniformly ^{13}C- and ^{15}N-labeled UTP, or [1′,6-$^{13}C_2$, 5-^{2}H]-UTP, respectively. The RNA in **d** can be prepared by solid-phase synthesis with a [1′,6-$^{13}C_2$, 5-^{2}H]-uridine amidite. Pink residues are isotope-labeled. Pink circles, cyan squares, and D represent ^{13}C, ^{15}N, and ^{2}H atoms, respectively.

Fig. 2 Examples of previously prepared isotope-labeled CEM [31] and TBDMS amidites [21], as well as the featured nucleobase and ribose labeled CEM amidite of the present study. Pink circles and D represent ^{13}C and ^{2}H atoms, respectively.

Figure 1

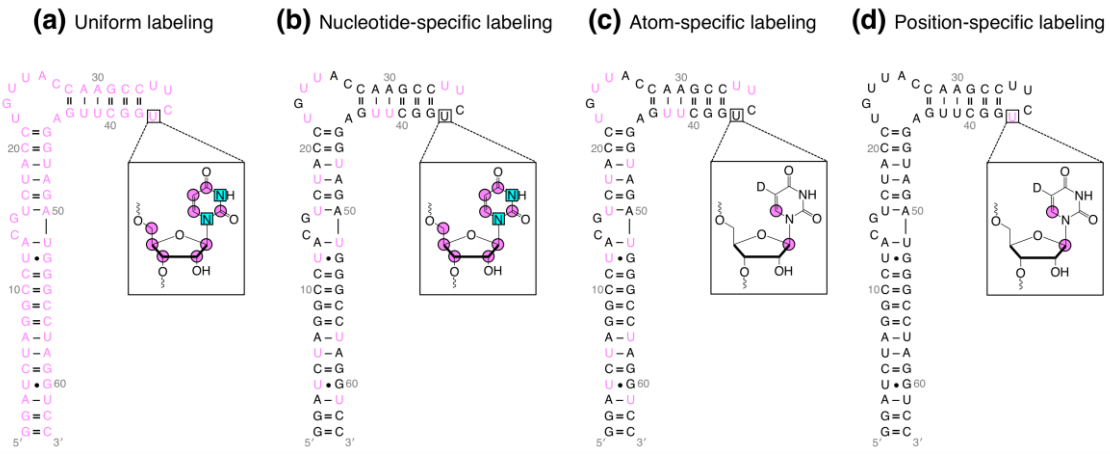

1

2

3 *Figure 2*

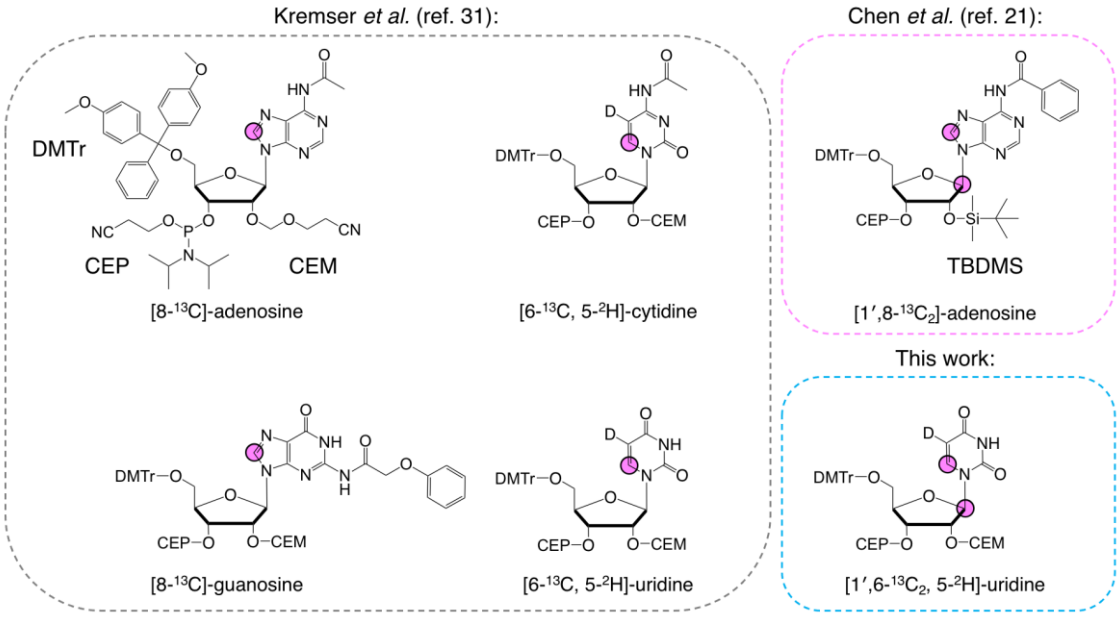

4

5

6 *Scheme 1*

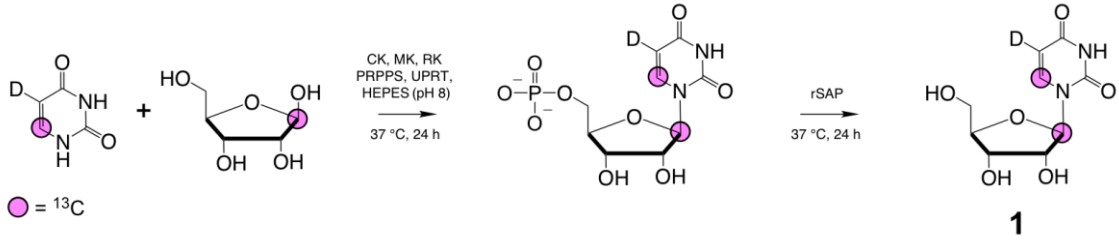

7

Scheme 2

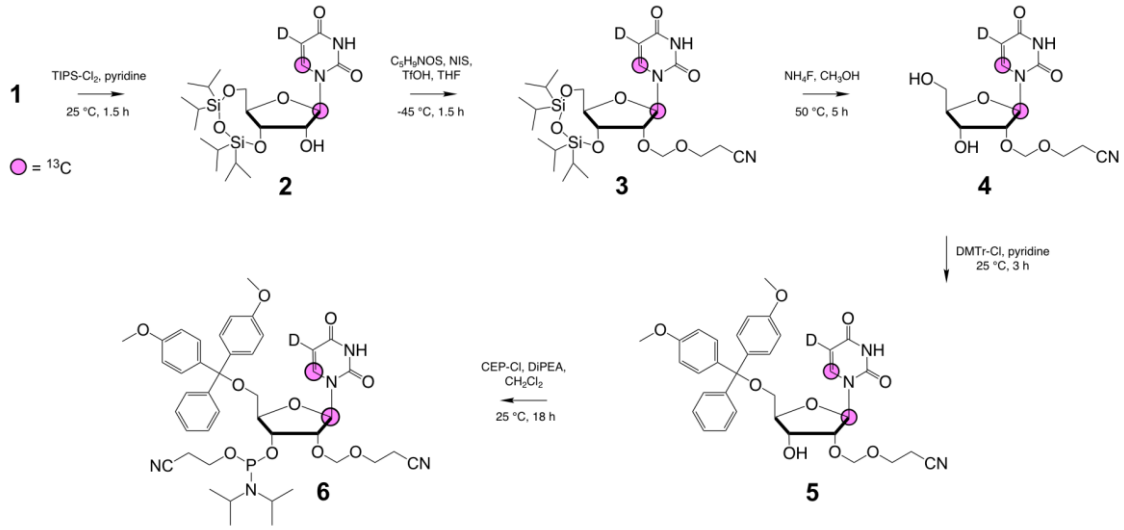

Graphical abstract